pH Determination Under Unconventional Conditions of Temperature and Ionic Strength

Ricardo G. Martínez−Pérez, Emmanuel Ruiz−Villalobos, Fernando D. González−Arteaga, Elizabeth Vilchis−Barrera, Jorge Ruvalcaba−Juárez, Arturo García−Mendoza*

Laboratorio de Química en Disolución y Electroquímica. Facultad de Estudios Superiores Cuautitlán, Universidad Nacional Autónoma de México, Cuautitlán Izcalli, Edo. de México, 54740, México.

*Corresponding author: Arturo García−Mendoza, email: arturogm@unam.mx

Abstract. The pH in an aqueous solution is a relevant parameter in many fields of chemistry, and its determination is not trivial when factors such as temperature and ionic strength are considered. In multicomponent systems, this situation becomes significant. Even in simple systems, there are variations of up to 1.813 pH units in CH_3COOK solutions when thermodynamic constants are used instead of apparent constants to calculate it. In this study, we propose a methodology that investigates the influence of these variables on the apparent dissociation constants of water and acetic acid, as well as their impact on the pH measurement of solutions prepared from CH_3COOH and a salt of its conjugate base. Non−linear adjustments were carried out using a polynomial analogous to the Van't Hoff equation to establish a relationship between the thermodynamic constants of formation and the wide temperature range proposed. Furthermore, the influence of the ionic medium was considered when correcting the activity coefficients using the extended model of the Debye−Hückel equation. This approach enabled a detailed description of the set of apparent formation constants, which were directly applied in the formal pH calculation without approximations. These variations were represented on response surfaces and interpolated to the proposed operating conditions. The successful correlation between the theoretical results and those obtained experimentally through potentiometric measurements confirmed a harmonious relationship between both data sets. The described methodology offers a novel alternative for calculating pH in multicomponent systems, including real samples, in unconventional conditions of temperature and ionic strength.
Keywords: Chemical equilibria; apparent constant; pH determination; Van't Hoff; Debye−Hückel.

Resumen. El pH en una disolución acuosa es un parámetro relevante en muchos campos de la química, y su determinación no es trivial cuando se consideran factores como la temperatura y la fuerza iónica. En sistemas multicomponente, esta situación se vuelve significativa. Incluso en sistemas simples, existen variaciones de hasta 1.813 unidades de pH en disoluciones de CH_3COOK cuando se utilizan constantes termodinámicas en lugar de constantes aparentes para calcularlo. En este trabajo, se propone una metodología que indaga en la influencia de estas variables sobre las constantes de disociación aparentes del agua y del ácido acético, así como su impacto en la medición del pH de soluciones preparadas a partir de CH_3COOH y una sal de su base conjugada. Se realizaron ajustes no lineales utilizando un polinomio análogo a la ecuación de Van't Hoff para establecer una relación entre las constantes termodinámicas de formación y el amplio rango de temperaturas propuesto. Además, se consideró la influencia del medio iónico al corregir los coeficientes de actividad mediante el modelo extendido de la ecuación de Debye−Hückel. Este enfoque permitió una descripción detallada del conjunto de constantes de formación aparentes, que se aplicaron directamente en el cálculo formal del pH sin aproximaciones. Estas variaciones se representaron en superficies de respuesta y se interpolaron a las condiciones de operación propuestas. La correlación exitosa entre los resultados teóricos y los obtenidos

experimentalmente mediante mediciones potenciométricas confirmó una relación armoniosa entre ambos conjuntos de datos. La metodología descrita ofrece una alternativa novedosa para el cálculo del pH en sistemas multicomponentes, incluidas muestras reales, en condiciones no convencionales de temperatura y fuerza iónica.
Palabras clave: Equilibrio químico; constante aparente; determinación del pH; Van't Hoff; Debye−Hückel.

Introduction

The pH is an essential measurement in the fields of chemistry [1,2], engineering [3], biology [4–6], and medicine[7,8], to quote a few disciplines. This parameter is a fundamental indicator of the acidity or alkalinity of a solution, as its value is determined by the shifts in concurrent chemical equilibria associated with the analytes exhibiting acid−base properties and the solvent itself. Additionally, the values of apparent equilibrium constants are influenced by various factors, with temperature and ionic strength being prominent among them. The effect of temperature is described by the Van't Hoff relationship, and the impact of ionic strength is addressed through the correction of activity coefficients using the Debye−Hückel equations[9, 10]. However, the interaction and interdependency between these factors are not always explicitly accounted for when calculating the pH value. In some educational practices, it has been observed that apparent equilibrium constants are considered invariant, given their name, leading to the misconception that pH and apparent equilibrium constants maintain the same values under all operating conditions, particularly those often described at $T = 25.0$ °C and $I = 0.0$ mol L^{-1} in the literature. Such practices can mislead students and result in their lack of understanding regarding unconventional measurements of these parameters [11–13]. These misconceptions have a profound impact on the conceptual understanding. Consequently, regardless of the application of apparent constants (whether in experimental terms, methodological design, or data analysis), rigorous control of temperature and prevailing ionic strength conditions is necessary. While ionic strength is the paramount parameter for adjusting the ionic character of the medium, this work includes sections related to salinity to circumvent the iterative algebraic expressions for water density.

It must be emphasized that the role played by pH is crucial for the quantification of substances and the optimization of complex chemical systems. Its mastery and appropriate application are essential for chemistry development across multiple disciplines, from scientific research to industry. For instance, the determination of pH in marine environments necessitates high ionic strength values ($I \geq 0.7226$ mol L^{-1}) and temperatures ranging from 4 to 50 °C [14]. Conversely, determining the pH of acetic acid solutions as brines requires high ionic strength and ambient temperature.

Although the variation of apparent equilibrium constants as a function of temperature and salinity in 3D domains has been previously examined, these have been numerical adjustments that lacked a chemical explanation for the employed fitting parameters [15].

In this study, an enhancement in the understanding of this phenomenon is presented through a methodology that allows for the precise calculation of the pH value of a solution defined by an analytical concentration (C_0) and subjected to specific temperature and ionic strength conditions. Two specific cases were analyzed: (1) a solution prepared from the acidic chemical species of the conjugate pair and (2) a solution prepared from the basic chemical species of such conjugate pair. Initially, the value of the apparent autoprotolysis constant of water (K_w) and an acidity constant (K_a) were obtained by incorporating the effects of temperature and ionic strength expressed in terms of salinity (Sp [PSU]). Such values were used to construct response surfaces, illustrating the variation of these constants over a wide range of operating conditions. The values that form these surfaces were then employed to create the pH response for the solutions mentioned above within a 3D space. Finally, the values obtained from this theoretical study were compared to some experimental pH measurements in solutions of acetic acid and sodium acetate prepared at $C_0 = 0.1$ mol L^{-1} and evaluated over selected temperature and ionic strength ranges. The correlation between theoretical and experimental pH values demonstrates a unitary slope, thus providing the possibility of applying the described method in subsequent determinations under unconventional temperature and ionic strength conditions.

Experimental

Reagents

Glacial acetic acid (CH$_3$COOH, Monterrey, C $\geq$ 16.94 mol L^{-1}) and potassium acetate (CH$_3$COOK, Aldrich, p $\geq$ 99 %) were employed as the acid−base conjugate pair under investigation and as the buffering medium for calibration. Potassium nitrate (KNO$_3$, Aldrich, p $\geq$ 99 %) was used to set the ionic strength values, and potassium hydroxide (KOH, J.T. Baker, p $\geq$ 98 %) as the titrant for alkalinization.

Deionized water ($\rho \geq$ 18.2 MΩ cm^{-1}, Milli−Q) was used to prepare all solutions and rinsing procedures. Potentiometric measurements were conducted under a nitrogen atmosphere (4.8 N$_2$, ProSpec, p $\geq$ 99.998 %) using a gas−washing glass bottle as a wetting chamber.

Instruments

Potentiometric measurements were conducted using a pH meter (model 785 DMP Titrino, Metrohm®, Swiss) connected to a combined glass electrode (model 6.0228.000, Metrohm®, Swiss). A previously calibrated water circulator (model 9105, PolyScience, USA) was employed and connected to the cells to maintain the working temperature. Masses were measured using a Mettler balance (XP105DR, $\pm$ 0.01 mg, Mettler Toledo, Swiss). Gravimetric and volumetric errors typically remained below 1.0 %.

Software

The R software (R Development Core Team, V 4.3.1) was employed for modeling response surfaces containing the values of apparent chemical equilibrium constants and pH, evaluated at specific ranges of temperature and salinity. Conventional calculations were performed using Microsoft Excel® 2023 spreadsheet software.

Theoretical response surfaces

To estimate the pH variation of a solution while maintaining a fixed initial concentration (C$_0$) under specific conditions of temperature, T [°C], and salinity, Sp [PSU], a methodology was developed, which can be summarized in two general steps. First, the logarithmic values of the apparent formation constants corresponding to the water formation constant $\left(\beta_{1,1}^{OH^-|H^+} = \frac{1}{K_w}\right)$ and the formation constant associated with a generic conjugate pair (HA/A$^-$) $\left(\beta_{1,1}^{A^-|H^+} = \frac{1}{K_a}\right)$, were obtained for defined temperature (4.0 $\leq$ T [°C] $\leq$ 100.0) and salinity (0.0 $\leq$ Sp [PSU] $\leq$ 70.0) ranges. Subsequently, these $\beta_{1,1}^{OH^-|H^+}$ and $\beta_{1,1}^{A^-|H^+}$ values were used in a third−degree polynomial to determine the effective molar concentration of solvated hydronium, [H$^+$], and subsequently, the pH of the proposed solution. A detailed description of the nomenclature used in this work to denote the formation constants is provided in Appendix A, Supporting Information [16].

Potentiometric measurements

Calibration of the combined glass electrode was carried out for four different ionic strength conditions (I$_1$ = 0.10 mol L^{-1}, I$_2$ = 0.20 mol L^{-1}, I$_3$ = 0.36 mol L^{-1}, and I$_4$ = 0.72 mol L^{-1}) and five temperature conditions (T$_1$ = 20.0 °C, T$_2$ = 25.0 °C, T$_3$ = 30.0 °C, T$_4$ = 35.0 °C and T$_5$ = 40.0 °C). A calibration curve was generated for each combination of these ionic strength and temperature values. For each of these curves, three buffer solutions were used, composed of (a) a HNO$_3$ solution with a C = 0.1000 mol L^{-1}; (b) an CH$_3$COOH/CH$_3$COO$^-$ buffer solution of equimolar concentrations to ensure that pH = pK$_a$; and (c) a KOH solution with C = 0.1000 mol L^{-1}.

For its preparation, first, the values of the apparent dissociation constants corresponding to K$_w$ and K$_a$(CH$_3$COOH/CH$_3$COO$^-$) were determined at the temperature and ionic strength conditions required for each situation mentioned above, using the methodology proposed in this work. Subsequently, the equilibrium concentration of the ionic species within the acid−base conjugated pairs H$_3$O$^+$/H$_2$O, CH$_3$COOH/CH$_3$COO$^-$ and H$_2$O/OH$^-$ respectively were calculated. Furthermore, the individual contributions of these species to the respective reaction media were determined in terms of ionic strength. These equilibrium concentrations were determined by solving the system of equations that results from considering the charge balance, the mass balance, and the acidity constants of the acid-base pairs involved [17–20]. Since KNO$_3$ is a true electrolyte, the equilibrium concentration of its ions in solution corresponds to its initial analytical concentration. Hence, it

became feasible to attribute the disparity between the targeted ionic strength value and that originating from the conjugate acid-base pair to a concentration of KNO_3 (and subsequently to its mass).

The masses of solid reagents and volumes of concentrated reagents were carefully measured and placed in a volumetric flask before reaching the volume mark using deionized water. After preparation, the solutions were standardized in the laboratory.

Theoretical study

Effect of temperature on thermodynamic constants

There are compilations of thermodynamic constants for various chemical equilibria [21–25]. While most of these pertain to isolated values, it is possible to describe their continuous variation concerning temperature using a Van't Hoff−type equation (Eq. 1). This expression considers the effect of ΔC_p [J mol^{-1} K^{-1}] over the entire range of temperature values analyzed [26].

$$\log \beta°_{eq} = \log \left(\beta_{1,1}^{A^-|H^+} \right)\Big|_{I=0} = B - \frac{A}{T} + C \ln(T) \qquad \text{Eq. 1}$$

The terms A (Eq. 2), B (Eq. 3), and C (Eq. 4) are functions of both enthalpy ($\Delta_r H_{298.15K}$ [J mol^{-1}]) and entropy at 298.15 K ($\Delta_r S_{298.15K}$ [J mol^{-1} K^{-1}]). In the following expressions, R is the universal gas constant (8.314472 J mol^{-1} K^{-1}), and T is the temperature in [K].

$$A = \frac{\Delta_r H_{298.15\,K} - (292.15\,K)\Delta C_p}{R \ln(10)} \qquad \text{Eq. 2}$$

$$B = \frac{\Delta_r S_{298.15\,K} - (1 + \ln(298.15\,K))\Delta C_p}{R \ln(10)} \qquad \text{Eq. 3}$$

$$C = \frac{\Delta C_p}{R \ln(10)} \qquad \text{Eq. 4}$$

Although the Van't Hoff equation is often thought to describe a linear relationship between $\log \left(\beta_{1,1}^{A^-|H^+} \right)\Big|_{I=0}$ and temperature, in practice, this dependence is not linear [27]. Therefore, performing a non−linear fit between the theoretical values of thermodynamic constants and the inverse of the temperature will yield better determination coefficients (R^2).

Effect of ionic strength on apparent constant

The activity coefficients of the chemical species involved in a chemical equilibrium are related to temperature and the contribution of the ionic strength of the medium within the framework of the Debye−Hückel theory [28] (Eq. 5). This expression is suitable for application in solutions with high ionic strength values [29–31].

$$\log \gamma_i = \frac{(-1.824829238 \times 10^6)\left(\rho_{(T,S,0)}\right)^{\frac{1}{2}} (\varepsilon_r T)^{-\frac{3}{2}} (z_i)^2 \sqrt{I}}{\left(1 + \dfrac{(50.29158649)\left(\rho_{(T,S,0)}\right)^{\frac{1}{2}}}{\sqrt{\varepsilon_r T}} \left(A_i \sqrt{I}\right) \right)} \qquad \text{Eq. 5}$$

Where γ_i is the activity coefficient of the *i*−th chemical species participating in the chemical equilibrium, T is the temperature in [K], I is the ionic strength in [mol L^{-1}], ε_r is the relative permittivity of

water, A_i is the solvated ion radius in [Å], z_i is the charge of the ion in question, and $\rho(T,S,0)$ is the solvent density in [g mL^{-1}] as a non−linear function of temperature and ionic strength evaluated at a pressure of 1 atm.

Although the mentioned parameters are known, it is possible to present them solely in terms of salinity and ionic strength, as detailed in the following sections.

In Debye−Hückel type models, it is considered that neutral species mix ideally in solutions; their electrostatic interactions with real ions are minimal, and therefore, their activity coefficients are considered unitary, regardless of the concentration of other molecular species or ionic in the solution [32]. Consequently, their activities are equal to their effective molar concentrations.

Ionic strength as a function of practical salinity

In a general sense, the ionic strength, I [mol L^{-1}], can be described as a measure of the ionic character of the medium and is a function of the effective molar concentration of all ions present at equilibrium, as Eq. 6 describes in its first equivalence [20].

$$I = \frac{1}{2}\sum z_i^2[i^z] = \left(0.722627\,\frac{mol}{Kg_{H_2O}}\right)\left(\rho_{(T,S,0)}\,\frac{Kg_{H_2O}}{L_{H_2O}}\right)\left(\frac{Sp}{35.0}\right) \qquad \text{Eq. 6}$$

The second equivalence in Eq. 6 illustrates the dependence of ionic strength on temperature and practical salinity (Sp [USP]), as reported by Millero in his book titled Chemical Oceanography (page 68) for the calculation of the ionic strength in units of molality [33]. In this work, a term for the density of water (as a function of temperature and salinity) is included in Eq. 6 to allow the expression of ionic strength in units of molarity. Thus, there exists a conversion between salinity and ionic strength that is valid for each temperature value (Appendix B, Supporting Information).

Dependence of the dielectric constant on temperature

The dielectric constant of a solvent is related to its ability to solvate ionized solutes [34]. The larger the dielectric constant value of a solvent, the more polar its character becomes, indicating that the solvent becomes more polarizable. The temperature dependence of this variable is given by Eq. 7, where the temperature should be evaluated in [K] [35].

$$\varepsilon_r = 5321(T)^{-1} + 233.76 - 0.9297(T) + 0.1417 \times 10^{-2}(T)^2 + 0.8292(T)^3 \qquad \text{Eq. 7}$$

Dependence of the water density on temperature and salinity

The density of water was estimated using the expression employed by UNESCO [36] in two steps. First, the density of pure water is determined as a unique function of temperature, ρ_{H_2O} (Eq. 8).

$$\rho_{H_2O} = a_0 + a_1T + a_2T^2 + a_3T^3 + a_4T^4 + a_5T^5 \qquad \text{Eq. 8}$$

Where:
- $a_0 = 999.842594$
- $a_1 = 6.793953 \times 10^{-2}$
- $a_2 = -9.095290 \times 10^{-3}$
- $a_3 = 1.001685 \times 10^{-4}$
- $a_4 = -1.120083 \times 10^{-6}$
- $a_5 = 6.536332 \times 10^{-9}$

The value of ρ_{H_2O} is obtained in [kg m^{-3}], and it is suggested to divide it by 1000 (1000 kg m^{-3} = 1 g mL^{-1}) to obtain the property in [g mL^{-1}]. To incorporate the influence of salinity, a series of adjustment coefficients are used, which are, in turn, functions of temperature (Eq. 9).

$$\rho_{(T,S,0)} = \frac{\left(\rho_{H_2O} + B_1S + C_1S^{1.5} + d_0S^2\right)}{1000} \qquad \text{Eq. 9}$$

Where:

- $B_1 = b_0 + b_1 T + b_2 T^2 + b_3 T^3 + b_4 T^4$
  - $b_0 = 8.2449 \times 10^{-1}$
  - $b_1 = -4.0899 \times 10^{-3}$
  - $b_2 = 7.6438 \times 10^{-5}$
  - $b_3 = -8.2467 \times 10^{-7}$
  - $b_4 = 5.3875 \times 10^{-9}$
- $C_1 = c_0 + c_1 T + c_3 T^2$
  - $c_0 = -5.7246 \times 10^{-3}$
  - $c_1 = 1.0227 \times 10^{-4}$
  - $c_2 = -1.6546 \times 10^{-6}$
- $d_0 = 4.8314 \times 10^{-4}$

In this calculation, the determination of the compressibility module on the density of water has been omitted, as it assumes a standard atmospheric pressure of 1 atm.

Ionic radii

The solvated ion radii are selected depending on the chemical equilibrium under consideration [37]. Table 1 lists the values of ion radii used for constructing the surfaces for the formation equilibrium of water $\left(\beta_{1,1}^{OH^-|H^+}\right)$ and for the formation equilibrium of acetic acid $\left(\beta_{1,1}^{CH_3COO^-|H^+}\right)$ [37–39].

Table 1. Ion radii values for the chemical species involved in the formation equilibria of water and acetic acid.

Ion	Solvated ionic radii (Å)	Reference
H$^+$	1.41	[37]
OH$^-$	1.33	[38]
CH$_3$COO$^-$	1.62	[39]

Apparent constant definition

Every chemical equilibrium exhibits a correlation between its apparent constant (expressed in terms of effective molar concentrations, with units and valid for a specific ionic strength value, I > 0 mol L^{-1}) and the thermodynamic constant (expressed in terms of activities, dimensionless, valid for zero ionic strength, I = 0 mol L^{-1}, and corresponding to a limiting situation) [17]. As the activity coefficients relate the terms of activity and effective molar concentration as $a_i = \gamma_i$ [i], it is possible to estimate the thermodynamic constant from each apparent constant value and their respective activity coefficients evaluated at nonzero ionic strength conditions (Eq. 10) [20].

$$K^o = \left(\beta_{1,1}^{A^-|H^+}\right)\Big|_{I=0} = \left(\frac{1}{K_a}\right)\Big|_{I=0} = \left(\beta_{1,1}^{A^-|H^+}\Big|_{I>0}\right) \prod \left(((\gamma_i)^{\nu_i})|_{I>0}\right) \qquad \text{Eq. 10}$$

Where ν_i y γ_i are, respectively, the stoichiometric coefficient and activity coefficient of the i−th component of the chemical equilibrium. In order to obtain a generalized expression, the species of the acid−base conjugate pair corresponding to the equilibrium constants were denoted as HA for the acidic species and A$^-$ for the basic species. Thus, Eq. 10 can be rewritten in logarithmic terms for practicality to determine $\log\left(\beta_1^{A^-|H^+}\right)\Big|_{I\geq0}$ (Eq. 11).

$$\log\left(\beta_{1,1}^{A^-|H^+}\Big|_{I>0}\right) = \log\left(\beta_{1,1}^{A^-|H^+}\right)\Big|_{I=0} - \sum \nu_i \log(\gamma_i|_{I>0}) \qquad \text{Eq. 11}$$

pH determination using third−degree polynomials

The effective molar concentration of the proton, [H⁺], was determined through the deduction of two third−degree polynomials that depend on the acid formation constant of the conjugate pair $\left(\beta_1^{A^-|H^+} = \frac{1}{K_a}\right)$ and the formation constant of water $\left(\beta_1^{OH^-|H^+}\right)$. The first polynomial is derived from a situation in which only the acid serves as the source of matter in the solution (Eq. 12).

$$[H^+]^3 + K_a[H^+]^2 - (K_w + K_aC_0)[H^+] - K_aK_w = 0 \qquad \text{Eq. 12}$$

In contrast, the second polynomial considers that a potassium salt of the conjugate base is responsible for providing the matter in the solution (Eq. 13). Potassium is an extremely weak acid that does not form hydroxo complexes due to its interaction with the solvent, so the participation of these chemical entities is neglected [26].

$$[H^+]^3 + (K_a + C_0)[H^+]^2 - K_w[H^+] - K_aK_w = 0 \qquad \text{Eq. 13}$$

Although trivial, the pH value corresponds to the logarithm of the effective molar concentration of the proton, pH = −log[H⁺]. It is calculated using the roots of the preceding polynomials that satisfy [H⁺] ∈ ℝ⁺. The detailed deduction of these polynomials is presented in Appendix C, Supporting Information [17,18,20]. These polynomials consider the contribution of all the chemical species present, regardless of their predominance in the medium, for calculating pH.

Results and discussion

Apparent formation constant of water as a function of temperature and salinity

Table 2 presents the values of the logarithms of the thermodynamic constants (I = 0 mol L⁻¹) for the formation equilibrium of water, reported at various temperature values [26,30,40,41].

Table 2. Collection of values of the logarithm of the water formation constant (numerically equal to pK$_w$) at zero ionic strength.

Temperature [°C]	$\log\left(\beta_{1,1}^{OH^-|H^+}\Big|_{I=0}\right) = pK_w\big|_{I=0}$	Reference
0.0	14.950	[26,40]
10.0	14.535	[26]
20.0	14.167	[26]
25.0	13.997	[26,41]
30.0	13.830	[26]
40.0	13.535	[26]
50.0	13.262	[40]
60.0	13.020	[30]
70.0	12.800	[30]
80.0	12.610	[30]
90.0	12.430	[30]
100.0	12.270	[30,40]

These values are presented *vs.* 1/T, as shown in Fig. 1 for a temperature range $(0.0 \leq T \,[°C] \leq 100.0)$. The non−linear fit of the data was carried out using the Solver® tool, included in Microsoft Excel® 2023, optimizing the value of the coefficient of determination R^2 [42] as an indicator of goodness of fit [43]. It was found that $\Delta C_p = 264.17$ J mol^{-1} K^{-1}, $\Delta_r H_{298.15K} = -57\,563.93$ J mol^{-1}, and $\Delta_r S_{298.15K} = 74.77$ J mol^{-1} K^{-1} [16]. The relative percentage difference with respect to the reported values is presented in Table S1 of Appendix D, Supporting Information. The estimation of thermodynamic parameters may vary depending on what was reported, because of the differences in the structure of the polynomials used for linear or non-linear fits and the width of the temperature intervals under study.

As the water formation equilibrium is typically exothermic $(\Delta_r H_{298.15K} < 0)$, the water autoionization equilibrium is an endothermic process that shifts towards products as the temperature increases; consequently, the pH of chemically pure water (where $[H^+] = [OH^-]$ with the omission of any additional ionic interaction) would change from 7.38 to 6.07 as the temperature increases within the studied range. There are reports within this range that numerically coincide with the calculated values [44].

While the relationship $\log\left(\beta_{1,1}^{OH^-|H^+}\big|_{I=0}\right)$ *vs.* 1/T is a straight line with a positive slope, the standard enthalpy value changes significantly to $\Delta_r H° = -52{,}087.82$ J mol^{-1}, with a coefficient of determination of less than $r^2 < 0.99$, which raises questions about these results compared to the proposed ones (results not shown).
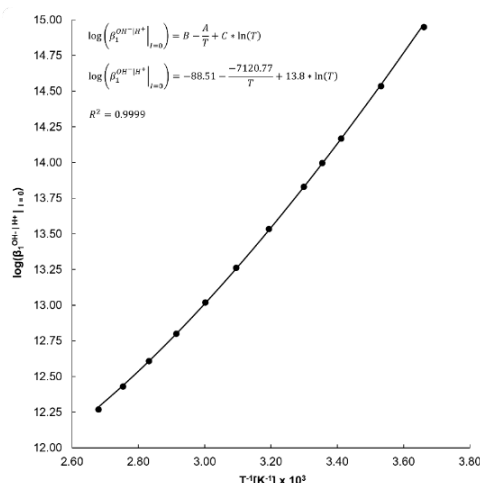

Fig. 1. Variation of the logarithm of the thermodynamic formation constant $(I = 0$ mol L$^{-1})$ for the $H^+ + OH^- \rightleftarrows H_2O$ equilibrium according to a non−linear Van't Hoff type model.

Eq. 14 describes the influence of the ionic medium on the water formation equilibrium. The activity coefficients presented in such expression use temperature and ionic strength as independent variables, allowing for their presentation in a 3D space after changing the variable in terms of salinity.

$$\log\left(\beta_{1,1}^{HO^-|H^+}\big|_{I>0}\right)$$
$$= \log\left(\beta_{1,1}^{OH^-|H^+}\big|_{I=0}\right) - \left(v_{H_2O} \times \log\left(\gamma_{H_2O}\big|_{I>0}\right)\right)$$
$$- \left(v_{H^+} \times \log(\gamma_{H^+}\big|_{I>0})\right) - \left(v_{OH^-} \times \log(\gamma_{OH^-}\big|_{I>0})\right) \qquad \text{Eq. 14}$$

In Appendix E, Supporting Information, a table is provided with the values of the apparent pK_w of water calculated for selected salinity and temperature values.
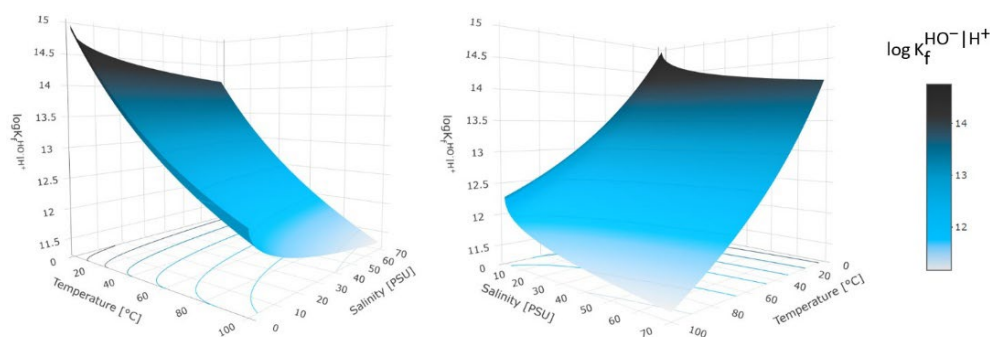
Fig. 2. Two perspectives of the response surface of the logarithm of the apparent formation constant for the H⁺ + OH⁻ ⇌ H₂O equilibrium within the proposed temperature (5.0 ≤ T[°C] ≤ 100.0) and salinity (0.0 ≤ Sp[PSU] ≤ 70.0) ranges.

In Fig. 2, it can be observed that the apparent constant associated with the water formation process decreases following a nearly linear trend as the temperature increases, as shown in the plane (log K vs. T). On the other hand, the decrease of this apparent constant with an exponential trend can be observed because of increasing salinity, as seen in the plane (log K vs. Sp). In accordance with Le Châtelier's principle, as the ionic strength of the medium increases, the chemical equilibrium shifts in the direction of increasing the number of formed ions corresponding to the products. Each point on the surface corresponds to a pK_w value, given for a set of coordinated pairs of salinity and temperature. This value limits the acid−base behavior in an aqueous solution under specific T and Sp conditions.

As reported by Martell & Smith [24], when T = 40 °C and S = 0 PSU, pK_w = 13.544, a value similar to the one presented on the surface in Fig. 2 (pK_w = 13.523), resulting in a relative percentage difference of 0.16 % when comparing the results.

Apparent formation constant of acetic acid as a function of temperature and salinity

The values of the logarithms of the thermodynamic constants (I = 0 mol L⁻¹) for the acetic acid formation equilibrium are presented in Table 3 [45].

Table 3. A collection of values of the logarithm of the acetic acid formation constant (numerically equal to $pK_a(CH_3COOH/CH_3COO^-)$), at zero ionic strength.

T [°C]	$\log\left(\beta_{1,1}^{CH_3COO^-\mid H^+}\Big\vert_{I=0}\right) = pK_a(CH_3COOH/CH_3COO^-)\vert_{I=0}$	Reference
0.0	4.7807	[45]
5.0	4.7696	[45]
10.0	4.7622	[45]
15.0	4.7582	[45]
20.0	4.7562	[45]
25.0	4.7559	[45]
30.0	4.7569	[45]
35.0	4.7625	[45]
40.0	4.7688	[45]

T [°C]	$\log\left(\beta_{1,1}^{CH_3COO^-|H^+}\Big|_{I=0}\right) = pK_a(CH_3COOH/CH_3COO^-)|_{I=0}$	Reference
45.0	4.7773	[45]
50.0	4.7870	[45]
55.0	4.7989	[45]
60.0	4.8119	[45]

These values are plotted *vs.* 1/T (Fig. 3) over a temperature range ($0.0 \leq T[°C] \leq 60.0$), where a non−linear optimization fit was carried out for R^2 [42, 43], revealing $\Delta C_p = 155.25$ J mol^{-1} K^{-1}, $\Delta_r H_{298.15K} = 440.48$ J mol^{-1}, and $\Delta_r S_{298.15K} = 92.52$ J mol^{-1} K^{-1} following the model in Eq. 1. The relative percentage differences compared to reported values are presented in Table S2 of Appendix D, Supporting Information [24, 45].

Fig. 3 shows the relationship of $\log\left(\beta_{1,1}^{CH_3COO^-|H^+}\Big|_{I=0}\right)$ *vs.* 1/T where a parabolic behavior with two identifiable ranges is apparent, one on each side of its axis. The first range occurs for $0.0 \leq T[°C] \leq 25.0$. As the temperature decreases from 25.0 °C, the values of $\log\left(\beta_{1,1}^{CH_3COO^-|H^+}\Big|_{I=0}\right)$ steadily increase, indicating an exothermic process ($\Delta_r H_{T<298.15K} < 0$). It is inferred that the dissociation of acetic acid is endothermic, suggesting that increasing the temperature favors it, causing the pH of an acetic acid solution to decrease as the temperature of the solution increases (up to 25 °C). The second range occurs for $25.0 \leq T[°C] \leq 60.0$. The temperature increments from 25.0 °C are accompanied by an increase in the values of $\log\left(\beta_{1,1}^{CH_3COO^-|H^+}\Big|_{I=0}\right)$, indicating this time an endothermic process ($\Delta_r H_{T>298.15K} > 0$). In this range, the dissociation of acetic acid is an exothermic process, so an increase in temperature would result in a decrease in the number of ions produced. Consequently, the pH of an acetic acid solution would increase as the temperature of the solution increases (from 20 °C). While these statements result from the analysis of Fig. 3, it should be noted that the influence of the ionic medium and the solvent dissociation constant have not been incorporated, so applying the descriptions mentioned above will not be valid for all operating conditions.

The relationship $\log\left(\beta_{1,1}^{CH_3COO^-|H^+}\Big|_{I=0}\right)$ *vs.* 1/T can only be applied in specific ranges of the dataset; extrapolating the linear relationship that appears at low temperatures would lead to significant discrepancies at temperatures above 25 °C.
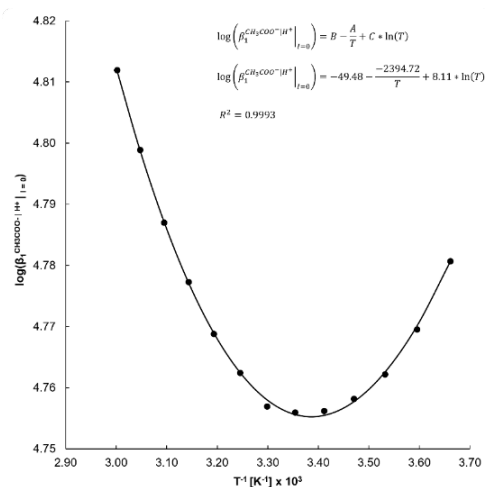

Fig. 3. Variation of the logarithm of the thermodynamic formation constant ($I = 0$ mol L^{-1}) for the equilibrium $CH_3COO^- + H^+ \rightleftarrows CH_3COOH$ according to a non−linear Van't Hoff−type model.

Fig. 4 shows the influence of the ionic medium on the acetic acid formation equilibrium (Eq. 15). In the log K *vs.* T plane, there is a negative exponential trend as the temperature decrease. In contrast, in the log K *vs.* Sp plane, the same trend is observed as salinity increases. Thus, the dissociation process of acetic acid tends to shift towards the ionic products as the salinity of the medium increases since the apparent value of $pK_a(CH_3COOH/CH_3COO^-)$ decreases. Consequently, the relative strength of acetic acid (strongly, moderately, or weakly dissociated) will depend on operational parameters beyond its concentration [46].

$$
\begin{aligned}
\log\left(\beta_{1,1}^{CH_3COO^-|H^+}\Big|_{I>0}\right) &= \log\left(\beta_{1,1}^{CH_3COO^-|H^+}\Big|_{I=0}\right) \\
&- \left(\nu_{CH_3COOH} \times \log\left(\gamma_{CH_3COOH}\Big|_{I>0}\right)\right) \\
&- \left(\nu_{H^+} \times \log(\gamma_{H^+}\big|_{I>0})\right) \\
&- \left(\nu_{CH_3COO^-} \times \log\left(\gamma_{CH_3COO^-}\Big|_{I>0}\right)\right)
\end{aligned}
\qquad \text{Eq. 15}
$$

According to the theoretical study conducted, the values of the apparent $pK_a(CH_3COOH/CH_3COO^-)$ for acetic acid range from a maximum of 4.748 for T = 5.0 °C and I = 1x10^{-6} mol L^{-1} to a minimum of 3.958 for T = 40.0 °C and I = 1.51 mol L^{-1}. A set of apparent $pK_a(CH_3COOH/CH_3COO^-)$ values for acetic acid is provided in Appendix F, Supporting Information, for selected salinity and temperature values.
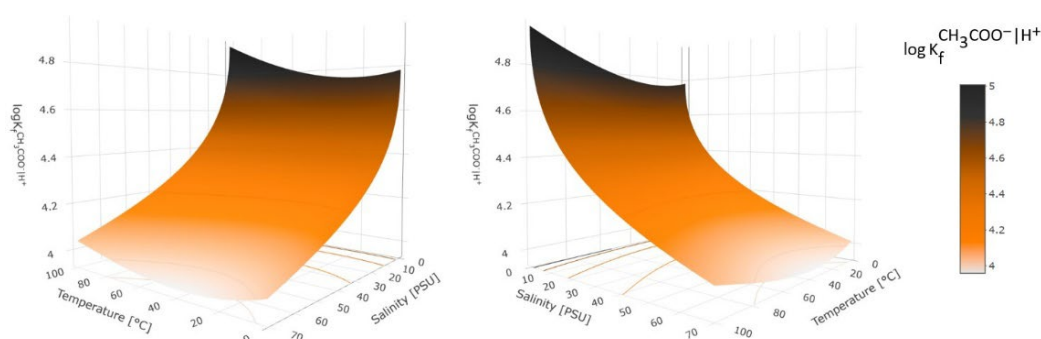
Fig. 4. Two perspectives of the response surface for the logarithm of the apparent formation constant for the equilibrium $CH_3COO^- + H^+ \rightleftarrows CH_3COOH$ within the proposed temperature ranges (0.0 ≤ T[°C] ≤ 60.0) and salinity (0.0 ≤ Sp[PSU] ≤ 70.0).

## Effect of temperature on pH determination

The pH of a solution prepared from acetic acid, $C_0 = 0.1$ mol L^{-1}, was calculated using the polynomial in Eq. 12, where an apparent equilibrium constant was assigned for each of the temperature and salinity values presented on the surface in Fig. 5. It can be observed that the pH is less sensitive to changes in ionic strength compared to the isolated value of its apparent pK_a. A maximum pH of 2.924 is observed at T = 70 °C and I = 0 mol L^{-1}, and a minimum pH of 2.486 at T = 40 °C and I = 1.51 mol L^{-1}, resulting in a difference of 0.437 pH units for the same test concentration. When considering the $pK_a°$ at T = 25 °C and calculating its value, an error of 10.2 % in underestimating [H$^+$] compared to the maximum value (pH = 2.923) and an error of 59.7% in overestimating [H$^+$] compared to the minimum value (pH = 2.486) would occur. For certain complex systems, these differences can lead to significant discrepancies. Appendix G in the Supporting Information presents the theoretical pH values of a solution prepared from acetic acid, $C_0 = 0.1$ mol L^{-1}, for selected salinity and temperature values.
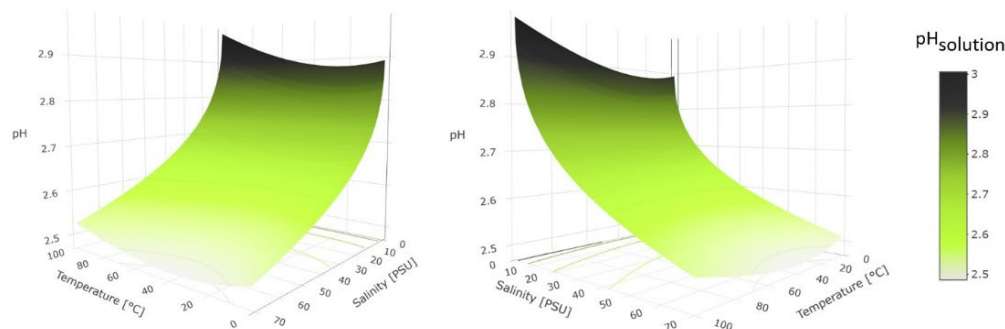
Fig. 5. Two perspectives of the response surface for the pH in an acetic acid solution with an initial concentration (C_0) of 0.1 mol L^{-1} within the proposed temperature ranges ($5.0 \leq T[°C] \leq 100.0$) and salinity ($0.0 \leq Sp[PSU] \leq 70.0$).

On the other hand, Fig. 6 presents the pH value of a solution prepared from potassium acetate, $C_0 =$ 0.1 mol L^{-1}, considering the effect of temperature and salinity on the constants that exhibit dependence on them. The formation equilibrium of the solution between the solvent and the salt of the alkali cation acetate is considered a total interaction, $KCH_3OO \rightarrow CH_3COO^- + K^+$ [47, 48]. Thus, the solvated conjugate base provides a reaction at equilibrium that allows the pH to be determined using Eq. 13.

On this surface, a maximum pH of 9.260 is observed at T = 0 °C and I = 0 mol L^{-1}, and a minimum pH of 7.447 at T = 70 °C and I = 1.49 mol L^{-1}, resulting in a difference of 1.813 pH units for the same solution. When the values of the thermodynamic constants $pK_a°$ and $pK_w°$ at T = 25 °C are used, a calculated pH value of 8.873 is obtained, which, when compared to the maximum and minimum values, is associated with an error by underestimating of 4.4 % in the pH with respect to the maximum value (pH = 9.260); and an error by overestimating of 16.1 % the pH concerning the minimum value (pH = 7.447). Other theoretical pH values for this solution are presented in Appendix H of Supporting Information.
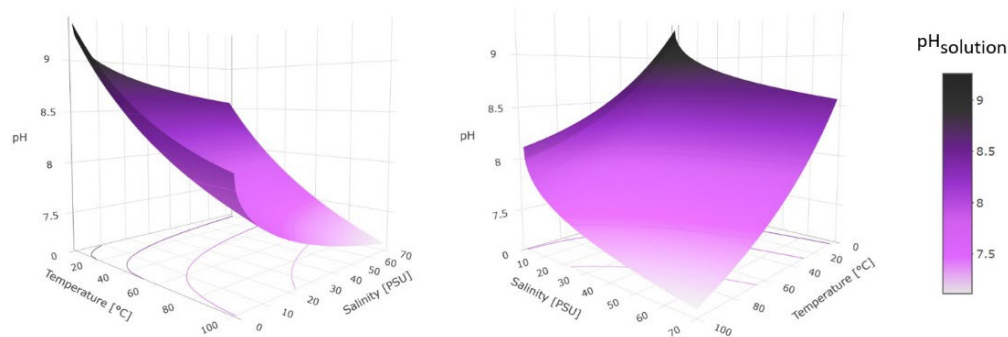

Fig. 6. Two perspectives of the response surface for the pH in a potassium acetate solution with an initial concentration (C_0) of 0.1 mol L^{-1} within the proposed temperature ranges ($5.0 \leq T[°C] \leq 100.0$) and salinity ($0.0 \leq Sp[PSU] \leq 70.0$).

Calculating pH using a polynomial without approximation provides better results than methodologies that assume predominant chemical entities to produce lower−order polynomials, which are only useful in reduced ranges within the 2D domain of $pK_a°$ *vs.* log (C_0), known as Gordus diagrams [46,49]. This kind of diagram fails because the ordinate axis would need to be readjusted for each temperature and salinity condition, and the equations that define the regions of separation of the reduced polynomials increase the error by at least 1.0%.

Fig. S2 in Appendix I of the Supporting Information shows these last two surfaces in the same 3D space. The upper part illustrates the pH value of a potassium acetate solution ($C_0 = 0.1$ mol L^{-1}), while the lower part shows this value for an acetic acid solution ($C_0 = 0.1$ mol L^{-1}). The temperature and salinity conditions for their respective maximum and minimum points do not coincide. Therefore, a gradual change in these two properties applied to a solution prepared from the conjugate acid and another prepared from the conjugate base would lead to different trends in terms of pH changes. Figure S3 shows the surface obtained by substracting one surface from the other (pH value of the potassium acetate solution and the pH value of the acetic acid solution) for each temperature and salinity condition at $C_0 = 0.1$ mol L^{-1}. This surface has a maximum pH of 6.372 at T = 0 °C and I = 0 mol L^{-1} and a minimum pH of 4.578 at T = 70 °C and I = 1.49 mol L^{-1}, resulting in a difference of 1.794 pH units between these two points for the same solution. This change differs substantially from the apparent pK$_a$ value of acetic acid for the proposed temperature and salinity ranges. Finally, in Figure S4, these two surfaces are compared. The upper surface corresponds to the difference in pH between the potassium acetate and acetic acid solutions, both at $C_0 = 0.1$ mol L^{-1}. In contrast the lower surface corresponds to the response of the logarithm of the apparent formation constant for the equilibrium $CH_3COO^- + H^+ \rightleftarrows CH_3COOH$ within the proposed temperature and salinity ranges. This surface emphasizes the importance of temperature and salinity control when mixing solutions to prepare a buffer solution. For conditions around T = 100 °C and I = 1.51 mol L^{-1}, the differences between the surfaces are not significant (%E=1.3 %). However, at conditions T = 0 °C and I = 1.51 mol L^{-1}, the differences become more relevant, resulting in a percentage error between the surfaces of 49.2 %.

Potentiometric assays

In Fig. 7 and Fig. 8, the correlation between the pH values obtained by potentiometric determination for CH$_3$COOH and CH$_3$COOK solutions with $C_0 = 0.1$ mol L^{-1} at specific temperature and salinity values and the pH values obtained using the methodology described in the theoretical study is presented.
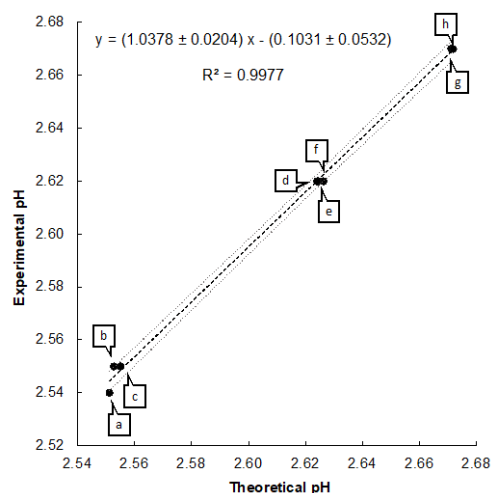
Fig. 7. Correlation between experimental pH values and values obtained by the methodology described in the theoretical study for an acetic acid solution, $C_0 = 0.1$ mol L^{-1}, at specific temperature (in °C) and salinity (in terms of ionic strength in mol L^{-1}) conditions for: (a) T = 35 °C, I = 0.72 mol L^{-1}; (b) T = 25 °C, I = 0.72 mol L^{-1}; (c) T = 20 °C, I = 0.72 mol L^{-1}; (d) T = 35 °C, I = 0.36 mol L^{-1}; (e) T = 25 °C, I = 0.36 mol L^{-1}; (f) T = 20 °C, I = 0.36 mol L^{-1}; (g) T = 30 °C, I = 0.2 mol L^{-1}; (h) T = 35 °C, I = 0.2 mol L^{-1}.

In both cases, the correlation between pH values tends towards a unitary slope. The temperature and salinity conditions used in the potentiometric determination of the pH are indicated for each point. It was observed that experimental determinations carried out at different temperature values tend to cluster concerning their ionic strength.

In Fig. 7, the linear function obtained has a slope of m = 1.0378 with an excellent correlation between experimental and theoretical values (R^2 = 0.9977). No biases were observed in the determinations for the replicates conducted (n = 3).
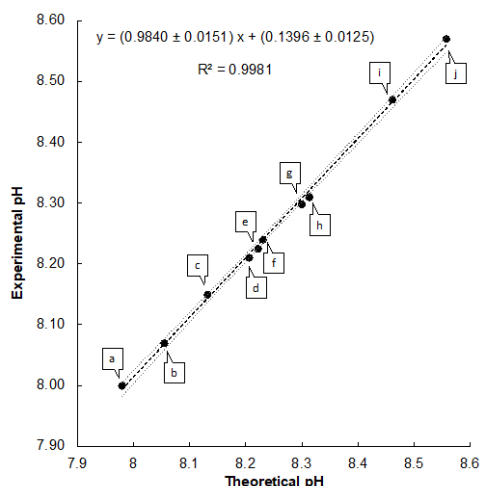
Fig. 8. Correlation between the experimental pH values and the values obtained using the methodology described in the theoretical study for a potassium acetate solution, C_0 = 0.1 mol L^{-1}, at specific temperature values (in °C) and salinity (in terms of ionic strength in mol L^{-1}) for: (a) T = 40 °C, I = 0.72 mol L^{-1}; (b) T = 35 °C, I = 0.72 mol L^{-1}; (c) T = 40 °C, I = 0.36 mol L^{-1}; (d) T = 25 °C, I = 0.72 mol L^{-1}; (e) T = 40 °C, I = 0.20 mol L^{-1}; (f) T = 20 °C, I = 0.72 mol L^{-1}; (g) T = 20 °C, I = 0.36 mol L^{-1}; (h) T = 25 °C, I = 0.20 mol L^{-1}; (i) T = 20 °C, I = 0.2 mol L^{-1}.

In Fig. 8, a slope of m = 0.9840 was obtained, with a slightly greater coefficient of determination than the previous case (R^2 = 0.9981). The choice of potassium salts for this solution helped reduce the alkaline error effect on the glass combined electrode [50]. These correlations support the possibility of applying the method in further experiments with a broader range of salinity and temperature values.

Before the potentiometric assays, measurements were carried out, setting the ionic strength with LiNO$_3$ (results not shown). It was observed that there was no significant difference in the determination of the pH property when using either LiNO$_3$ or KNO$_3$ to impose the ionic strength. The value of the K$^+$ interference potentiometric constant for the combined glass electrode used was also estimated, and it was found that its value tends to zero ($K_{K^+, pot} \leq 1 \times 10^{-11}$) [51]. If it were more significant, deformations would be observed at points h and g in Fig. 7, as well as points i and j in Fig. 8, due to the presence of the K$^+$ cation as an interferent leading to lower pH readings. If there is a significant potentiometric coefficient of interference of K$^+$ over H$^+$, a notable loss of linearity would be observed in alkaline environments on the lines presented in Fig. 7 and Fig. 8 affecting the correlation between the experimental pH values and the pH values obtained through the methodology proposed in this study.

The reader is invited to consult the Appendix J, Supporting Information, where hyperlinks to HTML−format files corresponding to the interactive 3D surfaces created using R® software are presented, as referenced throughout this article.

Conclusions

The construction of response surfaces to analyze the variation of pH as a function of temperature and ionic strength facilitates the joint representation of the interdependence that exists between the apparent dissociation constants of the acid-base pairs involved and the analytical concentration of the system, allowing

thus graphically visualize the magnitude of the impact that these variables exert on the pH. Non−linear fits were obtained using the Van't Hoff equation, allowing the determination of thermodynamic parameters such as $\Delta C_p°$, $\Delta_r H°$, and $\Delta_r S°$ for acetic acid and water. The obtained values showed a precision that did not significantly differ from those reported in the literature, being even better in some cases. Furthermore, a relationship between the values of thermodynamic formation constants and a wide range of temperatures was established. Additionally, the influence of the ionic medium was considered by correcting activity coefficients using the extended Debye−Hückel equation.

Finally, the experimental pH measurements showed a strong correlation with the pH values calculated using the proposed methodology, thereby supporting its reliability and accuracy. This rigorous and precise approach to pH determination in multicomponent systems has a beneficial impact on a wide range of applications, including research, practical applications, and education. The methodology presented here emerges as a resource to correct and elucidate experimental errors that often arise due to the oversimplification of models.

Acknowledgements

References

1. Buck, R. P.; Rondinini, S.; Covington, A. K.; Baucke, F. G. K.; Brett, C. M. A.; Camöes, M. F.; Milton, M. J. T.; Mussini, T.; Naumann, R.; Pratt, K. W.; Spitzer, P.; Wilson, G. S. *Pure Appl. Chem.* **2002**, *74*, 2169–2200.
2. Long, L.-S. *CrystEngComm.* **2010**, *12*, 1354–1365. DOI: https://doi.org/10.1039/b921146b.
3. Mayes, W. M.; Batty, L. C.; Younger, P. L.; Jarvis, A. P.; Kõiv, M.; Vohla, C.; Mander, U. *Sci. Total Environ.* **2009**, *407*, 3944–3957. DOI: https://doi.org/10.1016/j.scitotenv.2008.06.045.
4. Pierson, T. C.; Diamond, M. S. *Curr. Opin. Virol.* **2012**, *2*, 168–175. DOI: https://doi.org/10.1016/j.coviro.2012.02.011.
5. Tao, W.; Wang, J.; Parak, W. J.; Farokhzad, O. C.; Shi, J. *ACS Nano.* **2019**, *13*, 4876–4882. DOI: https://doi.org/10.1021/acsnano.9b01696.
6. Śmigiel, W. M.; Lefrançois, P.; Poolman, B. *Top. Life Sci.* **2019**, *3*, 445–458. DOI: https://doi.org/10.1042/etls20190017.
7. Abdella, S.; Abid, F.; Youssef, S. H.; Kim, S.; Afinjuomo, F.; Malinga, C.; Song, Y.; Garg, S. *Drug Dev. Ind. Pharm.* **2023**, *28*, 103414. DOI: https://doi.org/10.1016/j.drudis.2022.103414.
8. Hendi, A.; Hassan, M. U.; Elsherif, M.; Alqattan, B.; Park, S.; Yetisen, A. K.; Butt, H. *Int. J. Nanomed.* **2020**, *15*, 3887–3901. DOI: https://doi.org/10.2147/ijn.s245743.
9. Gigliuto, A.; Cigala, R. M.; Irto, A.; Felice, M. R.; Pettignano, A.; Milea, D.; Materazzi, S.; Stefano, C. D.; Crea, F. *Biomolecules.* **2021**, *11*, 1312. DOI: https://doi.org/10.3390/biom11091312.
10. Soleimani, F.; Afshari, T.; Mokhtari, F.; Gharib, F. *J. Chem. Thermodyn.* **2015**, *83*, 6–11. DOI: https://doi.org/10.1016/j.jct.2014.11.013.
11. Bellová, R.; Melicherčíková, D.; Tomčík, P. *J. Chem. Educ.* **2018**, *95*, 1548–1553. DOI: https://doi.org/10.1021/acs.jchemed.8b00086.
12. Clark, T. M.; Dickson-Karn, N. M.; Anderson, E. *J. Chem. Educ.* **2022**, *99* (4), 1587–1595. DOI: https://doi.org/10.1021/acs.jchemed.1c00819.

13. Styn, R.; Holtz, A.; Biselli, A.; Kaminski, S.; Jupke, A. *J. Solut. Chem.* **2022**, *51*, 517–539. DOI: https://doi.org/10.1007/s10953-022-01146-2.

14. Ma, J.; Shu, H.; Yang, B.; Byrne, R. H.; Yuan, D. *Anal. Chim. Acta.* **2019**, *1081*, 18–31. DOI: https://doi.org/10.1016/j.aca.2019.06.024.

15. Millero, F. J.; Graham, T. B.; Huang, F.; Bustos-Serrano, H.; Pierrot, D. *Mar. Chem.* **2006**, *100*, 80–94. DOI: https://doi.org/10.1016/j.marchem.2005.12.001.

16. Briones-Guerash-S. U.; García-Mendoza, A.; Aguilar-Cordero, J. C. *J. Chem. Educ.* **2023**, *100*, 4663–4673. DOI: https://doi.org/10.1021/acs.jchemed.3c00790.

17. Burgot, J. L., in: *Ionic Equilibria in Analytical Chemistry*, 1st ed.; Springer Science & Business Media, **2012**.

18. Butler, J. N.; Cogley, D. R., in: *Ionic Equilibrium: Solubility and pH Calculations*, 2nd ed.; John Wiley & Sons, Inc., **1998**.

19. Kahlert, H.; Scholz, F., in: *Acid-Base Diagrams*; Springer Science & Business Media, **2013**.

20. Castellan, G. W., in: *Physical Chemistry*, 3rd ed.; **1983**.

21. Martell, A. E.; Smith, R. M., in: *Critical Stability Constants. Volume 2: Amines*; Lenum Press, **1975**; Vol. 2. DOI: https://doi.org/10.1007/978-1-4613-4452-0.

22. Martell, A. E.; Smith, R. M., in: *Critical Stability Constants. Volume 3: Other Organic Ligands*; Springer Science+Business Media, **1977**; Vol. 3. DOI: https://doi.org/10.1007/978-1-4757-1568-2.

23. Martell, A. E.; Smith, R. M., in: *Critical Stability Constants. Volume 4: Inorganic Complexes*; Springer Science+Business Media, **1976**; Vol. 4. DOI: https://doi.org/10.1007/978-1-4757-5506-0.

24. Martell, A. E.; Smith, R. M., in: *Critical Stability Constants. Volume 5: First Supplement*; Springer Science+Business Media, **1982**; Vol. 5. DOI: https://doi.org/10.1007/978-1-4615-6761-5

25. Martell, A. E.; Smith, R. M., in: *Critical Stability Constants. Volume 6: Second Supplement*; Springer Science+Business Media, **1989**; Vol. 6. DOI: https://doi.org/10.1007/978-1-4615-6764-6.

26. Brown, P. L.; Ekberg, C., in: *Hydrolysis of Metal Ions*; John Wiley & Sons, **2016**.

27. Atkins, P.; de Paula, J., in: *Physical Chemistry*, 9th ed.; W. H. Freeman and Company, **2014**.

28. Gagliardi, L. G.; Castells, C. B.; Ràfols, C.; Rosés, M.; Bosch, E. *J. Chem. Eng. Data.* **2007**, *52*, 1103–1107. DOI: https://doi.org/10.1021/je700055p.

29. Helgeson, H. C.; Kirkham, D. H. *Am. J. Sci.* **1974**, *274*, 1199–1261. DOI: https://doi.org/10.2475/ajs.274.10.1199.

30. Fegley, B., in: *Practical Chemical Thermodynamics for Geoscientists*; Elsevier, **2013**.

31. Khan, M. N.; Warrier, P.; Peters, C. J.; Koh, C. A. *J. Nat. Gas Sci. Eng.* **2016**, *35*, 1355–1361. DOI: https://doi.org/10.1016/j.jngse.2016.03.092.

32. Burgot, J. L., in: *The Notion of Activity in Chemistry*, 1st ed.; Springer, **2016**.

33. Millero, F. J., in: *Chemical Oceanography*; CRC Press, **2016**.

34. Jouyban, A.; Soltanpour, S.; Chan, H.-K. *Int. J. Pharm.* **2004**, *269*, 353–360. DOI: https://doi.org/10.1016/j.ijpharm.2003.09.010.

35. Catenaccio, A.; Daruich, Y.; Magallanes, C. *Chem. Phys. Lett.* **2003**, *367*, 669–671.

36. Massel, S. R., in: *Internal Gravity Waves in the Shallow Seas*; Springer, **2015**. DOI: https://doi.org/10.1007/978-3-319-18908-6.

37. Marcus, Y. *Chem. Rev.* **2001**, *88*, 1475–1498.

38. Jenkins, B.; Thankur, K. P. *J. Chem. Educ.* **1979**, *56*, 576–577. DOI: https://doi.org/10.1021/ed056p576.

39. Roobottom, H. K.; Jenkins, H. D. B.; Passmore, J.; Glasser, L. *J. Chem. Educ.* **1999**, *76*, 1570. DOI: https://doi.org/10.1021/ed076p1570.

40. Bandura, A. V.; N, L. S. The *J. Phys. Chem. Ref. Data.* **2006**, *35*, 15–30. DOI: https://doi.org/10.1063/1.1928231.

41. Hunter, K. A., in: *Acid-base Chemistry of Aquatic Systems*, **1999**.

42. Brown, A. M. *Comput. Methods Programs Biomed.* **2001**, *65*, 191–200. DOI: https://doi.org/10.1016/S0169-2607(00)00124-3

43. de Levie, R., in: *How to Use Excel® in Analytical Chemistry and in General Scientific Data Analysis*; Cambridge University Press, **2001**.
44. Kiliç, E.; Aslan, N. *Microchim. Acta*. **2005**, *151*, 89–92. DOI: https://doi.org/10.1007/s00604-005-0380-1.
45. Harned, H. S.; Ehlers, R. W. *J. Am. Chem. Soc*. **1933**, *55*, 652–656. DOI: https://doi.org/10.1021/ja01329a027.
46. Gordus, A. A. *J. Chem. Educ*. **1991**, *68* 397. DOI: https://doi.org/10.1021/ed068p397.
47. Trémillon, B., in: *Chemistry in Non-Aqueous Solvents*; D. Reidel Publishing Company: Boston, USA, **1974**. DOI: https://doi.org/10.1007/978-94-010-2123-4.
48. Charlot, G.; Trémillon, B., in: *Chemical Reactions in Solvents and Melts*, First ed.; Harvey, D., Translator; Pergamon Press, **1969**.
49. Burke, J. D. *J. Chem. Educ*. **1976**, *53*, 79. DOI: https://doi.org/10.1021/ed053p79.
50. Boisen, O.; Corral, A.; Pope, E.; Goeltz, J. C. *J. Chem. Educ*. **2019**, *96*, 1418–1423. DOI: https://doi.org/10.1021/acs.jchemed.8b00812.
51. Bard, A. J.; Faulkner, L. R., in: *Electrochemical Methods*; Wiley, **2000**.